Supporting information

Graphene/MnO_2 aerogel with both high compression-tolerant ability and high capacitance for compressible all-solid-state supercapacitors

Peng Lv,* Xun Tang, Wei Wei

School of optoelectronic engineering, Nanjing University of Post & Telecommunications, Nanjing 210023, P. R China.

*Corresponding author: Email: lvp@njupt.edu.cn

Table 1 Mass contents and mass loadings of MnO_2 in graphene/MnO_2 aerogels with various deposition time.

Deposition time (min)	Mass content (wt%)	Mass loading (mg cm^{-2})
5	11	0.4
10	25	1.2
20	46	3.0
30	68	7.0
40	83	17.1

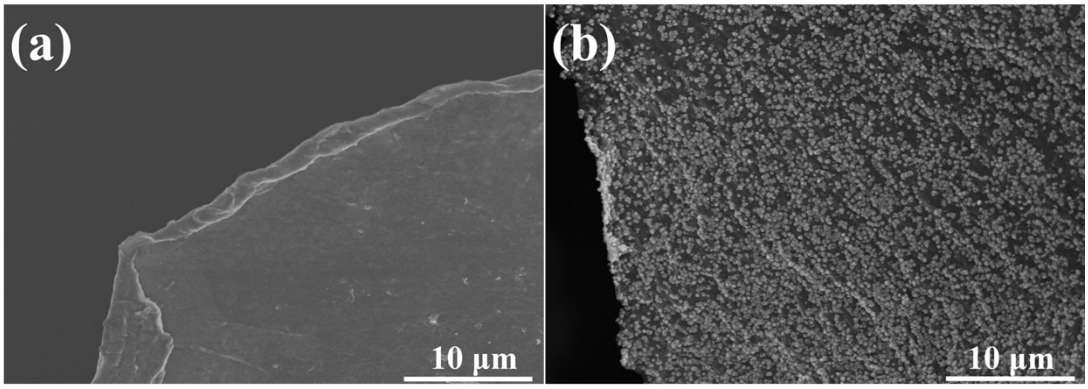

Fig. S1. SEM images of the cell walls of graphene aerogel (a) before and (b) after a 10-minute deposition process.

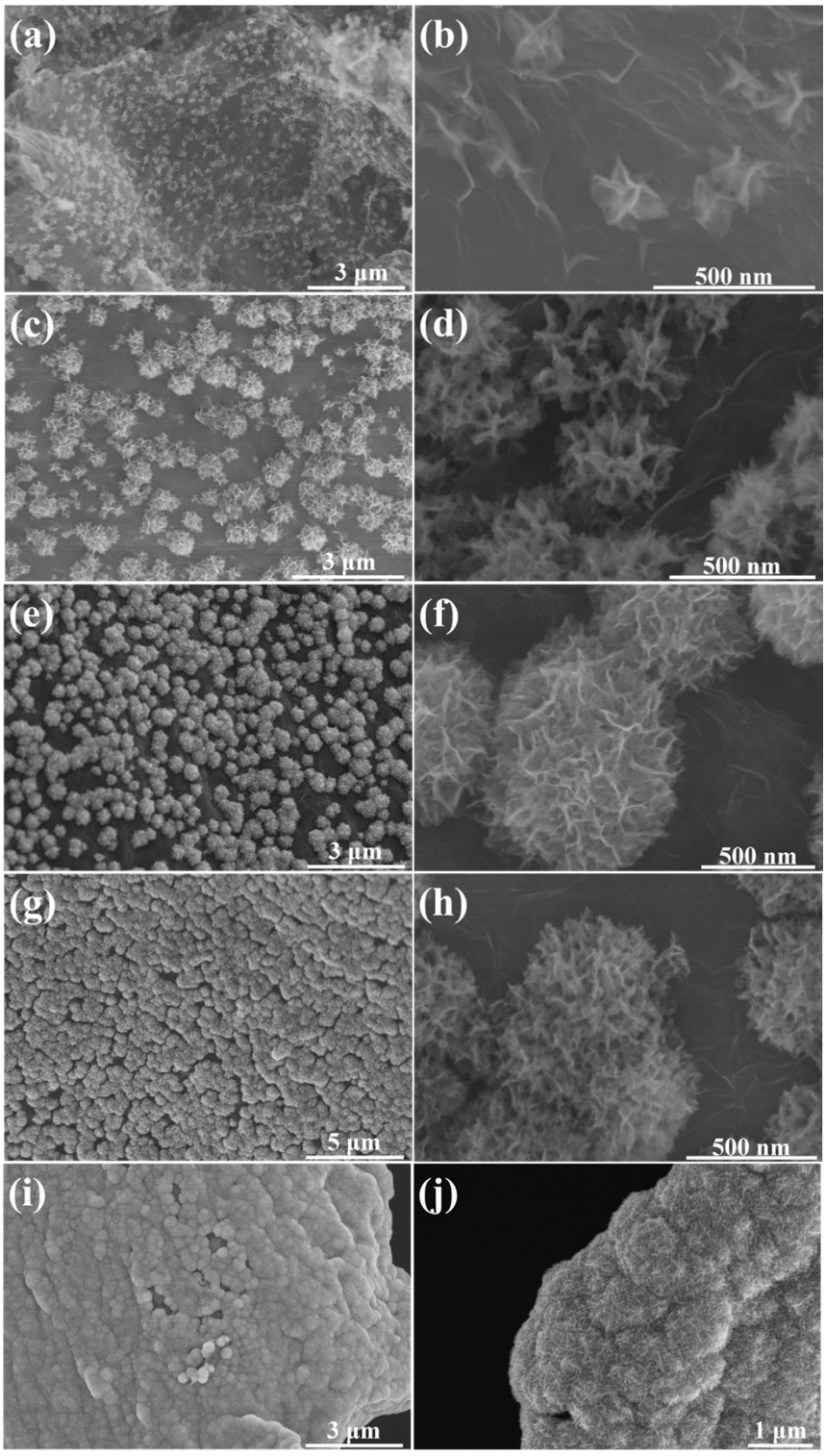

Fig. S2. SEM images of graphene/MnO_2 aerogel with the deposition time of (a, b) 5 min, (c, d) 10 min, (e, f) 20 min, (g, h) 30 min and (i, j) 40 min.

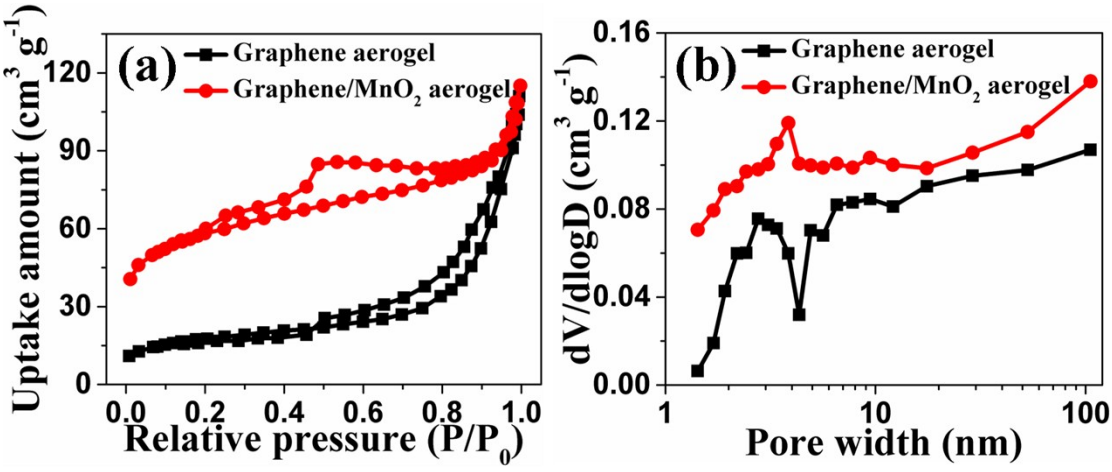

Fig. S3 (a) Nitrogen sorption isotherms and (b) pore size distribution of graphene aerogel and graphene/MnO_2 aerogel.

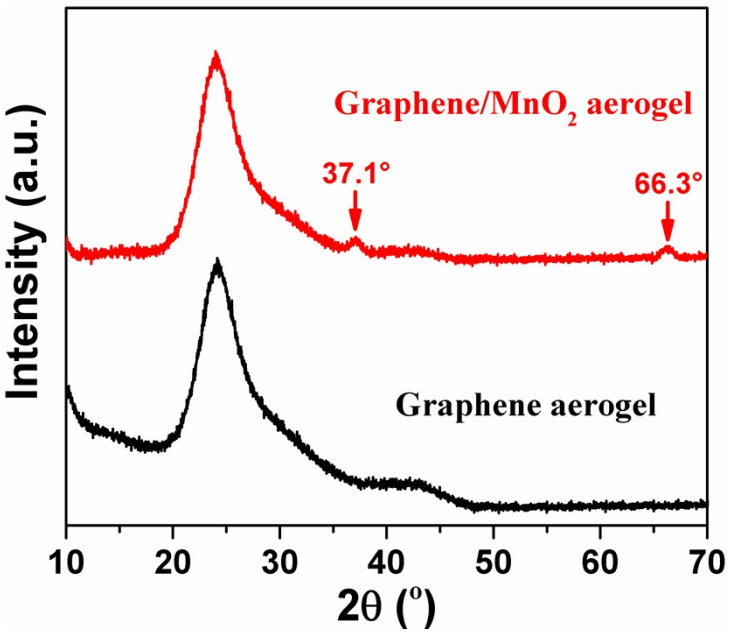

Fig. S4. X-ray diffraction (XRD) patterns of graphene/MnO_2 aerogel.

The two characteristic peaks at 37.1° and 66.3° in XRD analysis indicates the presence of MnO_2, and the weak, broad signals suggest that MnO_2 is amorphous nature, which is favorable for supercapacitor applications.

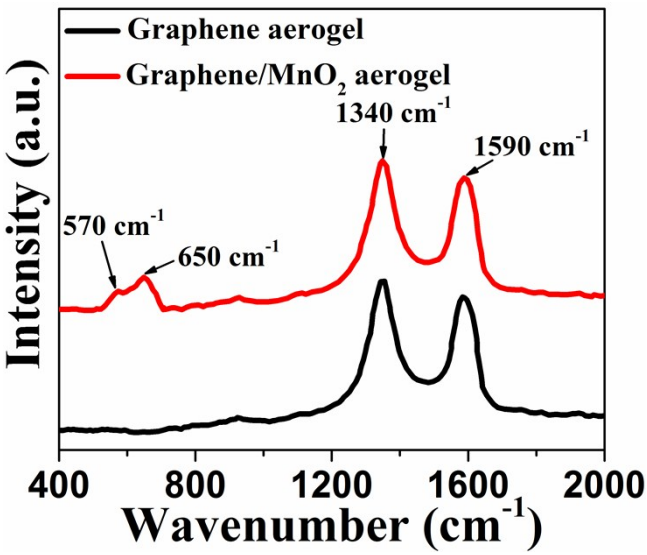

Fig. S5 Raman spectra of graphene aerogel and graphene/MnO_2 aerogel.

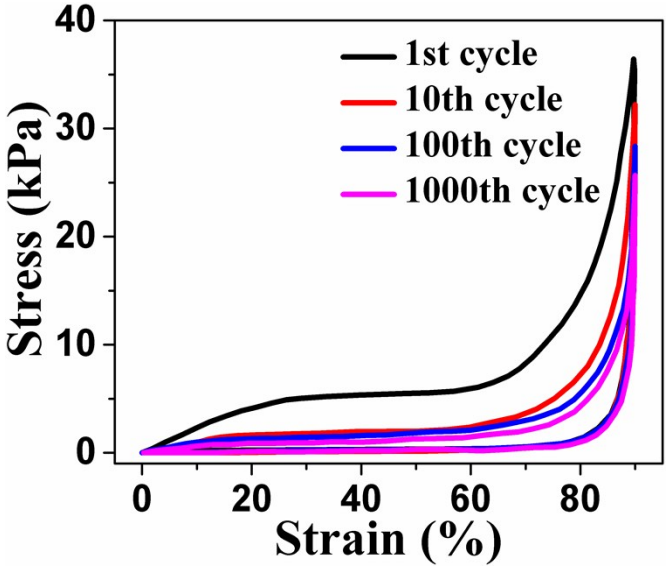

Fig. S6 Stress-strain curves of 1st, 10th, 100th and 1000th cycles of graphene aerogel at a set strain of 90%.

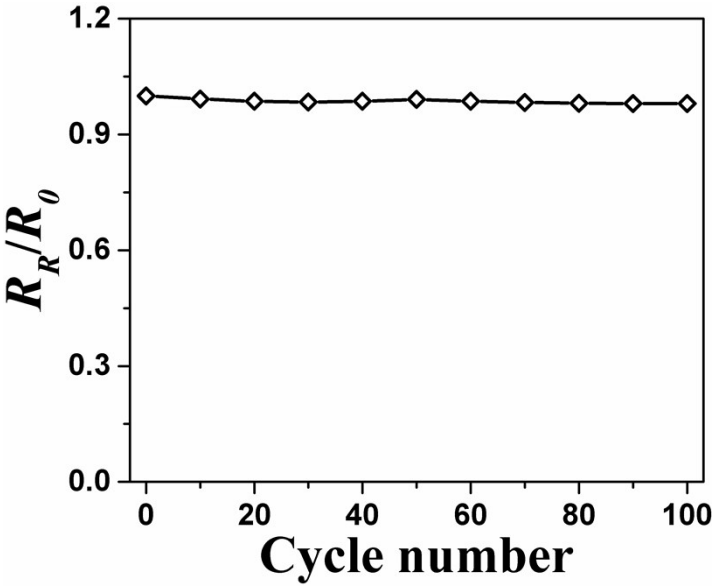

Fig. S7 The variation of electrical resistance of graphene/MnO_2 aerogel coated by PVA/H_2SO_4 in the first 100 compression-releasing cycles.

The electrochemical characterization of individual electrodes was carried out in three-electrode system with 1 M H_2SO_4 aqueous electrolyte. The as-prepared aerogel, Pt wire and Ag/AgCl were used as working electrode, counter electrode and reference electrode, respectively. To prevent any extraneous contribution to the capacity, the aerogel electrode was prepared by threading with a Pt wire without any other additive.

The specific capacitance of the aerogel electrode (C_s) was calculated from the cyclic voltammetry (CV) curves by using the equation: $C_s = \int \frac{I}{m} dU / v\Delta U$, where I is the response current, m is the mass of the aerogels (including graphene and MnO_2), v is the potential scan rate, ΔU is the potential range.

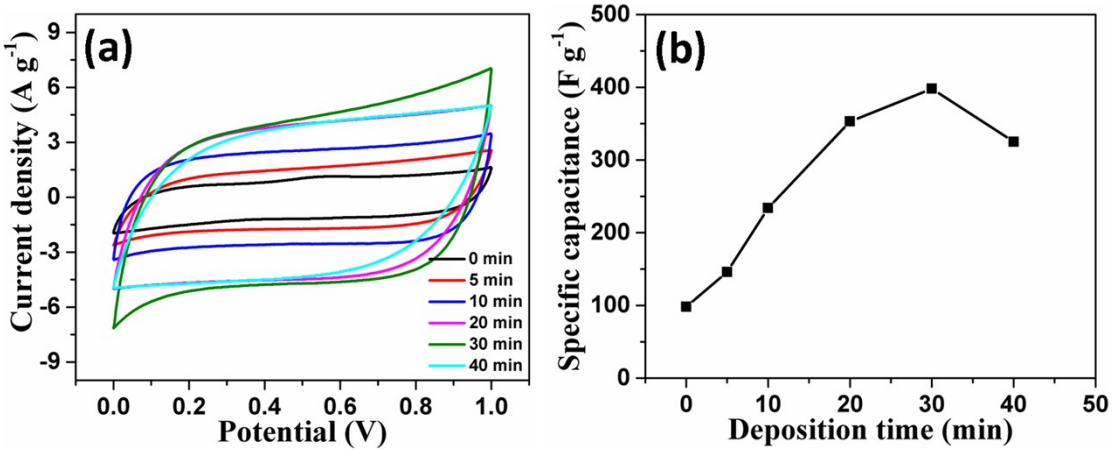

Fig. S8 (a) CV curves of the graphene/MnO_2 aerogels deposited for 0, 5, 10, 20, 30, and 40 min at 10 mV s^{-1}; (b) the specific capacitances of the aerogels calculated from the CV curves in (a).

The microstructure of CC before and after the deposition of MnO_2 is shown in Fig. S9. CC before the electrochemical deposition process shows a smooth surface (Fig. S9 a-c). After 30 min deposition of MnO_2, there are plenty of MnO_2 nanosheets coated on the surface of carbon fiber in CC. The specific capacitance of CC/MnO_2 was measured by cyclic voltammetry using a three-electrode system. CC/MnO_2 with MnO_2 mass loading of 4.2 mg cm^{-2} shows a specific capacitance of 224 F g^{-1} at 10 mV s^{-1}, which is lower than that of graphene/MnO_2 (398 F g^{-1}) with MnO_2 mass loading of 3.9 mg cm^{-2}. The relative high value of specific capacitance of graphene/MnO_2 is attributed to the unique characteristic of the graphene aerogel substrate: 1. The 3D network of graphene aerogel provides continuous conductive path for efficient electron transfer, thus reducing the internal resistance of the electrode; 2. Graphene aerogel provides larger surface area (72 m^2 g^{-1}) than that of CC (20 m^2 g^{-1}) for loading MnO_2. For the same mass loading, the thickness of MnO_2 on graphene cell walls is much lower than that on CC; 3. The interconnected macroporous structure of graphene aerogel favors the homogeneous deposition of MnO_2, avoiding the aggregation of MnO_2.

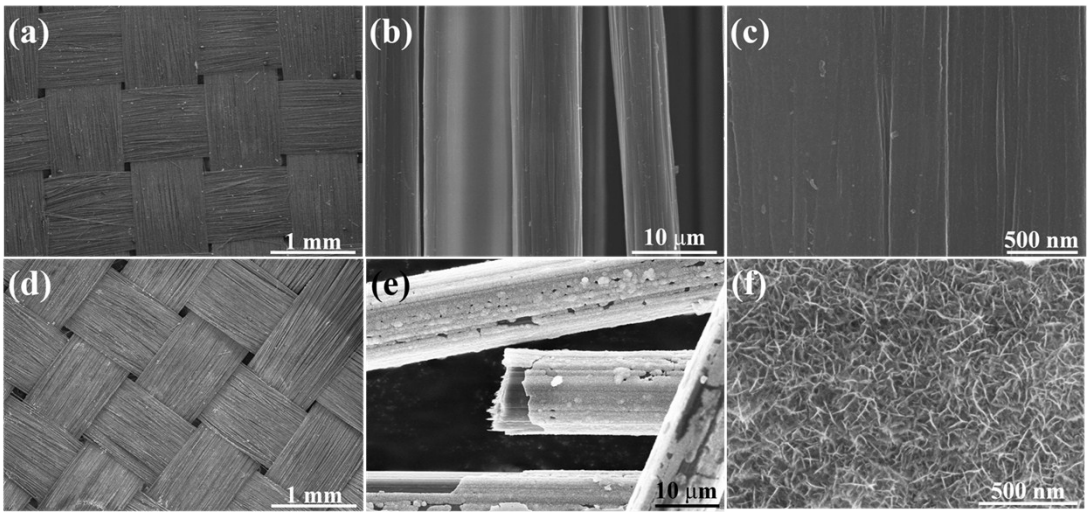

Fig. S9 SEM images with various magnifications of (a-c) CC and (d-f) CC/MnO_2.

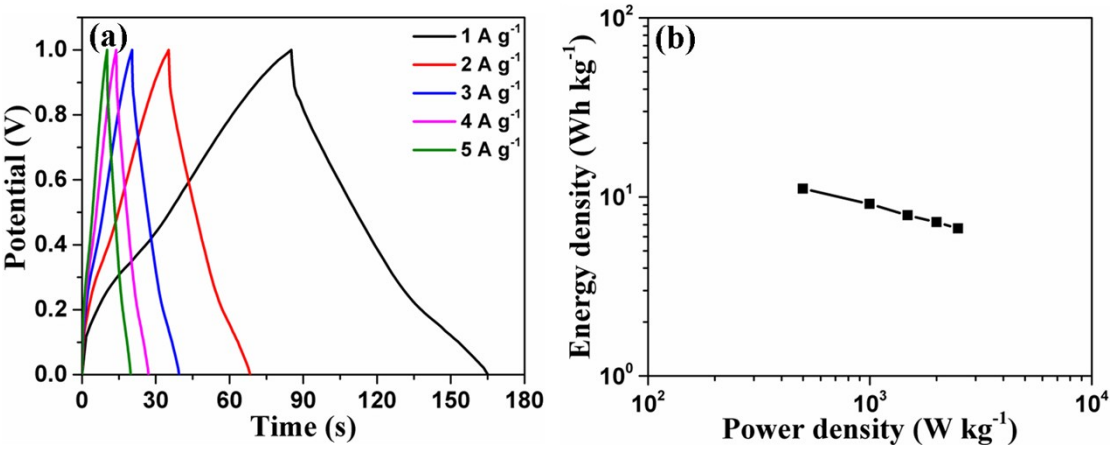

Fig. S10 (a) Galvanostatic charge/discharge curves at various current densities from 1 to 5 A g^{-1} and (b) Ragone plot of a representative all-solid-state compressible supercapacitor.